EJMSE

MICROSTRUCTURAL AND SUPERCAPACITIVE PERFORMANCE OF CUBIC SPINEL Li₄Ti₅O₁₂ NANOCOMPOSITE

Chandra Sekhar JINKA[1], Dhananjaya MERUM[1], Hussain OBILI MAHAMMAD[1,*]

[1]Thin film Laboratory, Department of Physics, Sri Venkateswara University, Tirupati, 517 502, India.

Abstract

Nanocrystalline $Li_4Ti_5O_{12}$ was synthesized using solid state reaction method. The influence of sintering temperature on chemical composition and microstructure was studied. The $Li_4Ti_5O_{12}$ powder sintered at 900 °C exhibited predominant (111) orientation representing cubic spinel structure with particle size of 46 nm. The composition and phase were confirmed from TG and EDX measurements. The displayed bright spots with clear diffracted rings in SAED pattern corresponding to characteristic orientations confirm the cubic spinel LTO phase. The pure LTO electrode exhibited a discharge specific capacitance of 265 F/g at current density of 0.5 A/g with good cycling stability (81%) after 5000 cycles. The significance electrochemical properties are attributed to the phase purity of LTO with low particle size which provides improved conduction paths.

Keywords*: nanocrystalline $Li_4Ti_5O_{12}$, solid state reaction, CV, GCD, supercapacitor*
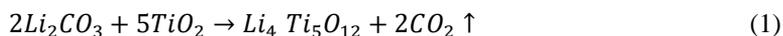
Introduction

In recent decades, the rapidly growing world energy demand has triggered enormous research efforts towards the design and development of advanced high energy density electrochemical energy storage (EES) systems. Among all EES devices, supercapacitors provide higher power density, fast recharge capability, and long cycle activity. The electrochemical performance of supercapacitors mainly depends on the microstructural features of active electrode material. A large number of electrode materials viz. Mixed metal oxides & hydrides, carbonaceous materials, conducting polymers have been used in the fabrication of supercapacitors. Particularly, the transition metal oxides evolved as potential materials due to natural abundance, low cost and incredible electrochemical properties combining with good structural stability [1-8]. Among all binary metal oxides, the spinel $Li_4Ti_5O_{12}$ (LTO) has been recognized as a potential candidate for energy storage devices owing to good structural stability and zero-strain throughout electrochemical process by preventing the decomposition of electrode and lithium dendrites formation. It delivers a high theoretical capacity (175 mAh g^{-1}) and shows a constant voltage plateau at 1.55 V (Li/Li$^+$). However, the electrochemical performance is constrained due to low electronic conductivity and lithium ion diffusion [8-13]. Several innovative methods such as doping, lowering crystallite size, carbon coatings on surface of the active material [14-16] have been employed to overcome these difficulties. One of the suitable ways to enhance the interfacial surface area of the active electrode material is to reduce particle size which in turn shorten the lithium ion diffusion path length and enhance the contact surface area of the electrode and electrolyte.

$Li_4Ti_5O_{12}$ has been synthesized by different chemical techniques such as sol-gel, molten salt, pyrolysis, microwave radiation, hydrothermal, and solid state reaction. Among all, solid state reaction method is a simple, widely used method and the precursors are inexpensive and abundant

Corresponding author: hussainsvu@gmail.com

[12, 15-18]. Recently several researchers reported the influence of synthesis process parameters on the physical and chemical properties of $Li_4Ti_5O_{12}$. For example, Deng et al. prepared $Li_4Ti_5O_{12}$ nanospheres and demonstrated high discharge capacity and better capacity retention [19]. Hydrothermally synthesized $Li_4Ti_5O_{12}$ hollow spheres exhibited a capacitance of 653 F/g at a current density of 1 A/g with good cycling stability [20]. The solid state reaction mechanism during the synthesis of $Li_4Ti_5O_{12}$ electrode was thoroughly studied by Shen et al. using PXRD and TG – DTA [21]. Ni et al. synthesized C - $Li_4Ti_5O_{12}$ nano composite using sol-gel process and demonstrated improved conductivity and electrochemical properties through reducing particle size [13]. The phase pure $Li_4Ti_5O_{12}$ and doped (Al^{3+}, Mg^{2+}, Cr^{3+}) $Li_4Ti_5O_{12}$ electrodes were synthesized by Lee et al. using solid state reaction and demonstrated its application in hybrid supercapacitors [12]. These results conclude that the phase purity, crystallite size, and electrochemical properties of $Li_4Ti_5O_{12}$ essentially depend on the process parameters. In the present study, nanocrystalline LTO has been synthesized using solid state reaction method and studied the influence of reaction temperature on the phase, microstructure, and electrochemical properties of synthesized $Li_4Ti_5O_{12}$ electrode for supercapacitor applications.

Materials and Methods

$Li_4Ti_5O_{12}$ nano-powders were prepared by solid state reaction method using 5:2 weight ratio of anatase titanium oxide (TiO_2) and lithium carbonate (Li_2CO_3) constituents. Sufficient amount of ethanol was poured into the mixture of raw precursors and grinded for 3 h. The obtained slurry was placed in a micro oven and dehydrated at 80 °C for 5 h. Moreover, the powder was sintered in a furnace at various reaction temperatures ranging from 700 °C to 900 °C for 5 h. The solid state chemical reaction mechanism during the synthesis process can be expressed by the following equation:

$$2Li_2CO_3 + 5TiO_2 \rightarrow Li_4\ Ti_5O_{12} + 2CO_2 \uparrow \tag{1}$$

The crystal structures of prepared $Li_4Ti_5O_{12}$ powders were described by Siefert X-ray diffractometer (XRD) – 303 TT. The XRD spectra were documented with Cu Kα radiation source in the angular range from 10º to 70° at a scan rate of 5 °/min. The physical and chemical changes of the blended precursor were studied by thermo gravimetric analysis using a Netzsch STA 449C in constant Ar to O_2 flow rate (heating rate of 1 °C/min). The microstructure and morphology of synthesized powders were characterized by Transmission and Scanning electron microscopes (HRTEM-FEI microscope – TECHNAIG2-30S-twin D905 and SEM - Carl Zeiss EVO50). The elemental composition of the synthesized $Li_4Ti_5O_{12}$ powder was observed by Energy Dispersive Spectrometer attached in the TEM column.

The electrochemical properties of the synthesized $Li_4Ti_5O_{12}$ were studied using an aqueous three electrode cell. A platinum strip, Ag/AgCl and optimized $Li_4Ti_5O_{12}$ electrode (sintered at 900 °C for 5 h) were used as the counter electrode, reference electrode and working electrode, respectively. The working electrode was made by systematically mixing of synthesized LTO, acetylene black, and poly vinylidene fluoride (PVDF) in the weight percentage of 80:10:10. The mixture was added with few drops of N-methyl-2-pyrrolidone to form slurry and uniformly distributed over the Ni substrates. Finally, the electrode was dried at 100 °C in a furnace for 3 h. 1 Mole of saturated lithium sulfate aqueous solution was used as electrolyte. The cyclic voltammetry (CV), galvanostatic charge-discharge (GCD) and electrochemical impedance

spectroscopy (EIS) analyses were conducted with CHI 608C electrochemical workstation in the potential window ranging from − 0.3 V to +0.5 V.

Results and Discussion

Fig. 1 shows the X-ray diffraction spectra of as synthesized $Li_4Ti_5O_{12}$ powder samples at different sintering temperatures. The XRD spectrum of the sample sintered at 700 °C shows an additional small anatase TiO_2 phase along with $Li_4Ti_5O_{12}$ phases which may be due to insufficient temperature for the completion of the reaction. Further increasing the sintering temperature to 800 °C, the XRD peaks of TiO_2 phase are disappeared and the peaks corresponding to cubic spinel $Li_4Ti_5O_{12}$ phase are appeared. The diffraction peaks presented at 2θ values of 18.30º, 35.48º, 43.18º, 47.38º, 57.25º, 62.77º, 66.13º are ascribed to (111), (311), (400), (331), (333), (440), (531) planes of cubic spinel $Li_4Ti_5O_{12}$ (JCPDS: 49-0207) with Fd$\overline{3}$m space group [13, 22-25]. Also, the intensity of the orientated XRD profiles increased with further increasing the sintering temperature to 900 °C.
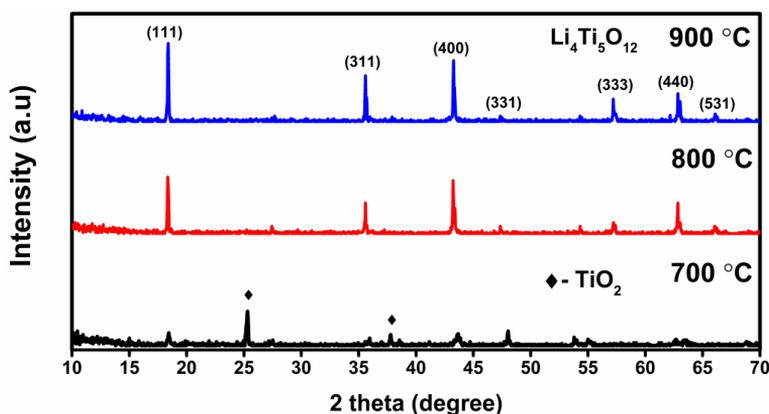

Fig. 1. XRD patterns of $Li_4Ti_5O_{12}$ sintered at different temperatures

The Scherrer's formula [$L = \frac{K\lambda}{B\cos\theta}$, where K is a dimensionless shape factor (0.9 for spherical particles), λ wavelength of the X-ray source, B the full-width at half maximum (FWHM), and θ the Bragg angle] was employed to calculate the crystallite size. The dislocation density (δ) [$\delta = \frac{1}{L^2}$] and unit volume (V) [$V = a^3$] were calculated and are summarized in Table 1.

Table 1. The crystallographic parameters as synthesized samples at different temperatures

T_s (°C)	Lattice parameters a (Å)	Grain size (nm)	Dislocation density 10^{10} cm^{-2}	Unit volume nm³
700	8.625(2)	28	12.7	641.61
800	8.532(2)	32	9.7	621.08
900	8.349(3)	46	4.7	581.97

The estimated lattice parameter value (a) from least square fit method and the unit volume of LTO synthesized at 900 °C is in good agreement with reported value indicating the formation of phase pure $Li_4Ti_5O_{12}$. The low crystallite size and high dislocation density in LTO sample synthesized at 700 °C indicates insufficient reaction temperature. The small crystallite size is

attributed to the large number of grain boundaries, which creates a free volume and produces a hydrostatic-like pressure which responsible for high stress and high dislocation densities for the samples prepared at lower temperatures (< 900 °C).

The TG analysis was carried from room temperature to 900 °C and is shown in Fig.2 to understand the possible chemical reaction between TiO_2 and Li_2CO_3 constituents in the field of thermal energy. The initial weight loss observed from R_T to around 300 °C is due to loss of absorbed water from the surfaces and ethanol during $Li_4Ti_5O_{12}$ synthesis. The TG curve show a step-like pattern of weight loss (15.20 %) during the heating process between 300 °C to 700 °C, which is nearly equal to the theoretical weight loss value (16.15 wt%) of carbon dioxide when escape from Li_2CO_3 [21, 22]. Further increasing the temperature from 700 °C to 900 °C, mass of the sample retains constant (+0.70%) representing the formation of crystalline $Li_4Ti_5O_{12}$ phase. The TG result is well coordinated with XRD analysis of the synthesized $Li_4Ti_5O_{12}$ phase.
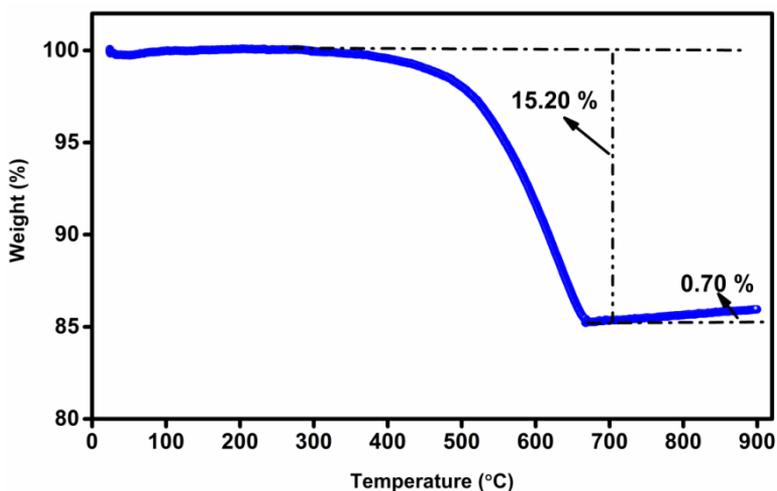

Fig. 2. TG analysis graph of *Li₄Ti₅O₁₂*

The SEM images of $Li_4Ti_5O_{12}$ powders synthesized at different sintering temperatures (700 °C, 800 °C and 900 °C) for 5 h in air atmosphere are shown in Fig. 3(a, c, e). In addition, the distributions of the relative particle size of these samples were expressed in statistical histograms and are depicting in Fig. 3(b, d, f). The micrographs displays that the shape and particle size of the synthesized powders were effectively influenced by the sintering temperature. The powder sintered at 700 °C (Fig. 3b) consists of a particle size distribution of 80 – 260 nm and a maximum number of particles between 100 to 120 nm. The powder prepared at 800 °C (Fig. 3d) constitutes a particle size range from 150 – 550 nm and major particles lying in the 200 – 250 nm. Moreover, the powder synthesized at 900 °C (Fig. 3f) has a long size ranging from 200 – 800 nm with more particles in the 400 to 500 nm range. Therefore, the particle size of prepared sample at 700 °C is smaller than the others samples due to incomplete reaction with led to the presence of additional TiO_2 (as per XRD) along with $Li_4Ti_5O_{12}$ phase. The $Li_4Ti_5O_{12}$ powder synthesized at 900 °C exhibited (Fig. 3e) the formation of uniformly distributed cubical grains and each grain is composed of several crystallites.

The High Resolution Transmission Electron Microscopy (HR-TEM) images and Selected Area Electron Diffraction (SAED) pattern of the sample synthesized at 900 °C are shown in Fig. 4(a, b and c). From figure 4.a, each cubic particle contains group of nanocrystallites and supports the SEM analysis. The synthesized $Li_4Ti_5O_{12}$ shows cubic spinel structure with a d- spacing value of 0.48 nm (Fig. 4 b) attributed to the (111) peak of XRD spectrum of $Li_4Ti_5O_{12}$ phase. The

calculated lattice parameter (a) was found to be 8.31 nm using measured d spacing and (111) orientation, also well supported to the XRD results. The SAED pattern (Fig. 4 c) displayed clear diffused rings with brighter spots demonstrating that synthesized $Li_4Ti_5O_{12}$ powder is in good crystalline state with each crystallite in nanometer scale. The rings of SAED pattern corresponding to the (111), (311), (440), (531) and (400) planes confirm the formation of cubic spinel $Li_4Ti_5O_{12}$ phase [26, 27]. The elemental composition of synthesized compound was surveyed using EDS analysis and is illustrated in Fig. 5. The EDS spectrum displayed Ti and O elements at their relevant binding energy positions with atomic weight of 18.65 and 81.35 respectively. Due to low characteristic radiation, Li element cannot be identified from EDAX spectrum [2].
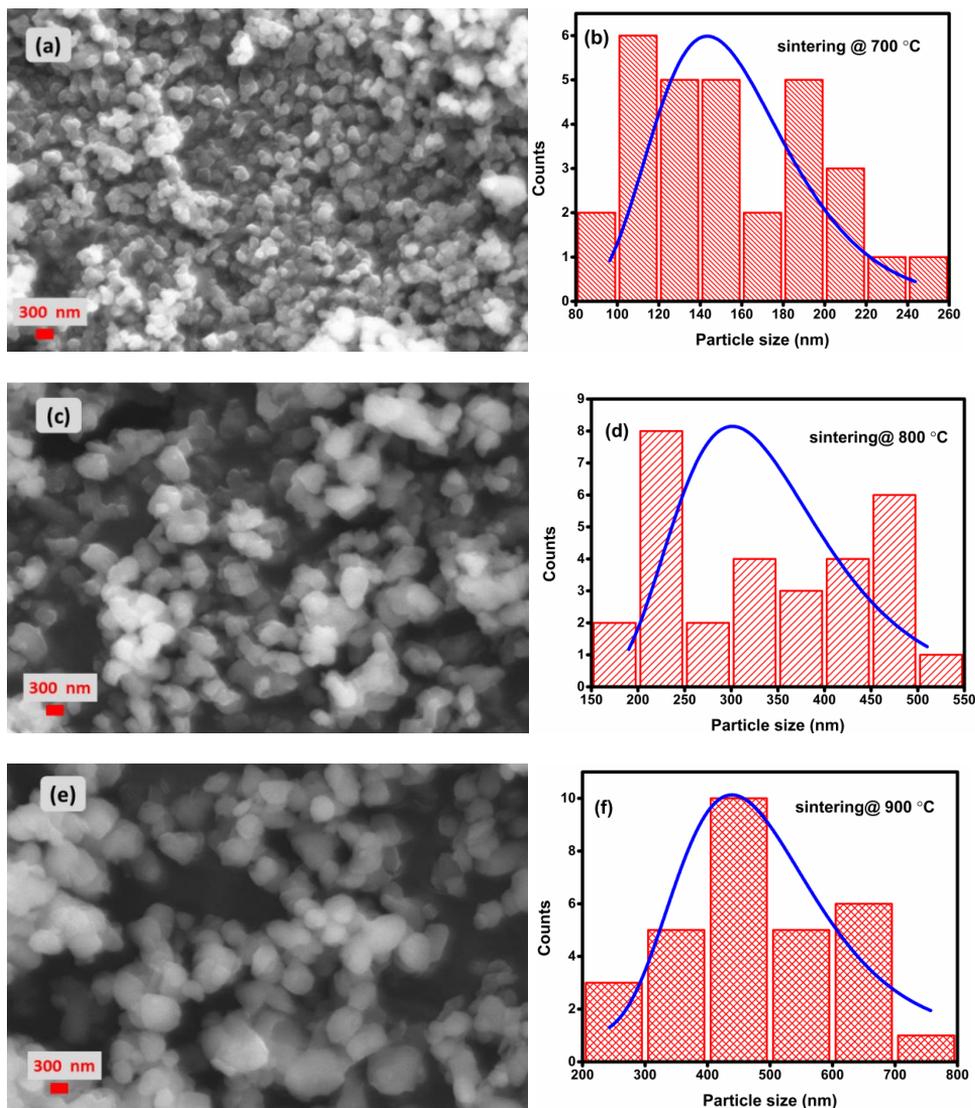

Fig. 3. Microstructural analysis and particle size distribution: a), c), e) SEM images of $Li_4Ti_5O_{12}$ (sintered at 700 °C, 800 °C and 900 °C); b), d), f) their resultant statistical histogram for particle size distribution

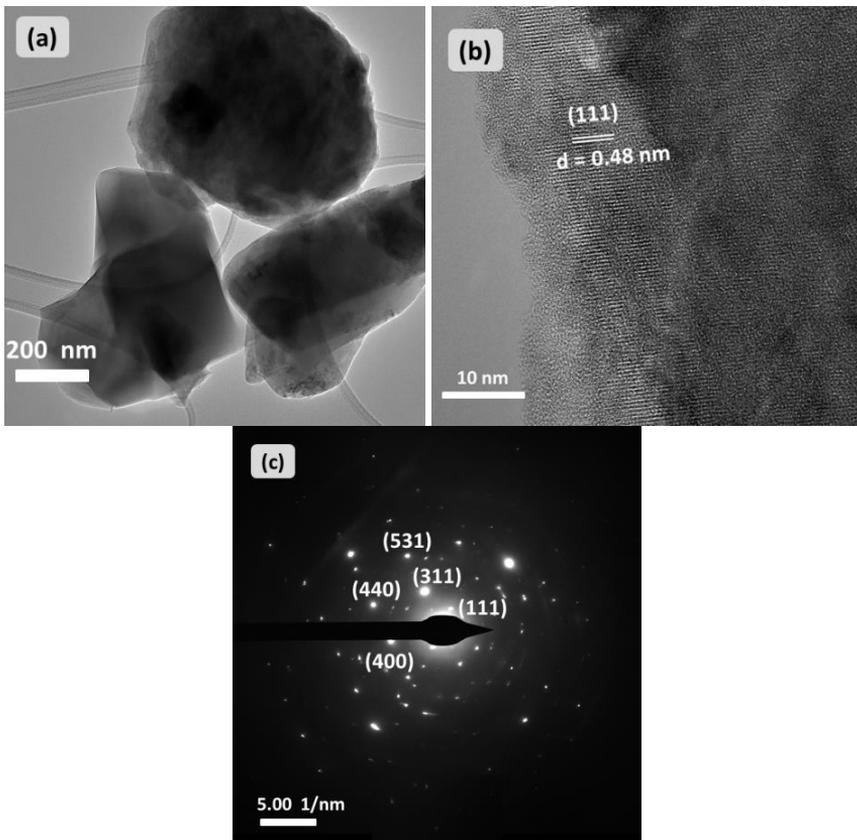**Fig. 4.** Microstructural analysis: a), b) HRTEM images; c) SAED pattern of Li$_4$Ti$_5$O$_{12}$

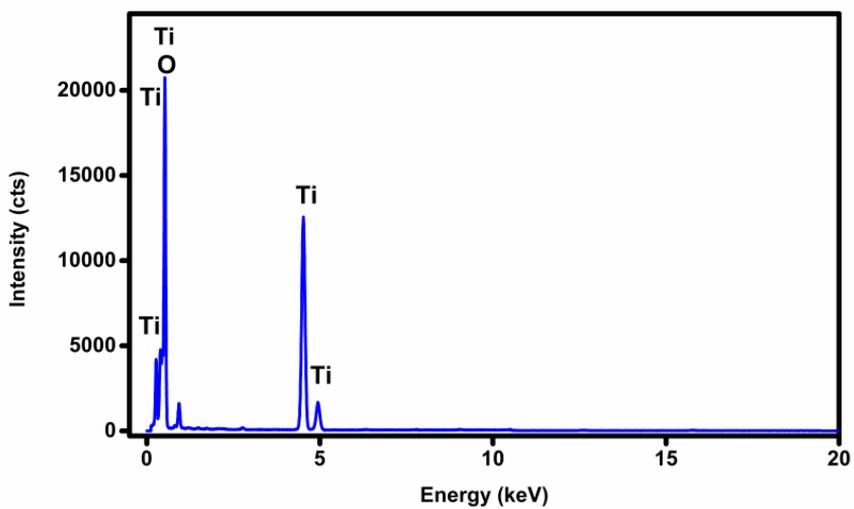**Fig. 5.** EDS spectrum of Li$_4$Ti$_5$O$_{12}$

The elemental mapping images of the nanocrystalline LTO were found using high angle angular dark field scanning transmission electron microscopy (HAADF) and are shown in Fig. 6.

The particles are uniformly distributed with Ti and O elements and characteristic X-rays emit from their respective positions confirm the chemical homogeneity of $Li_4Ti_5O_{12}$ phase.

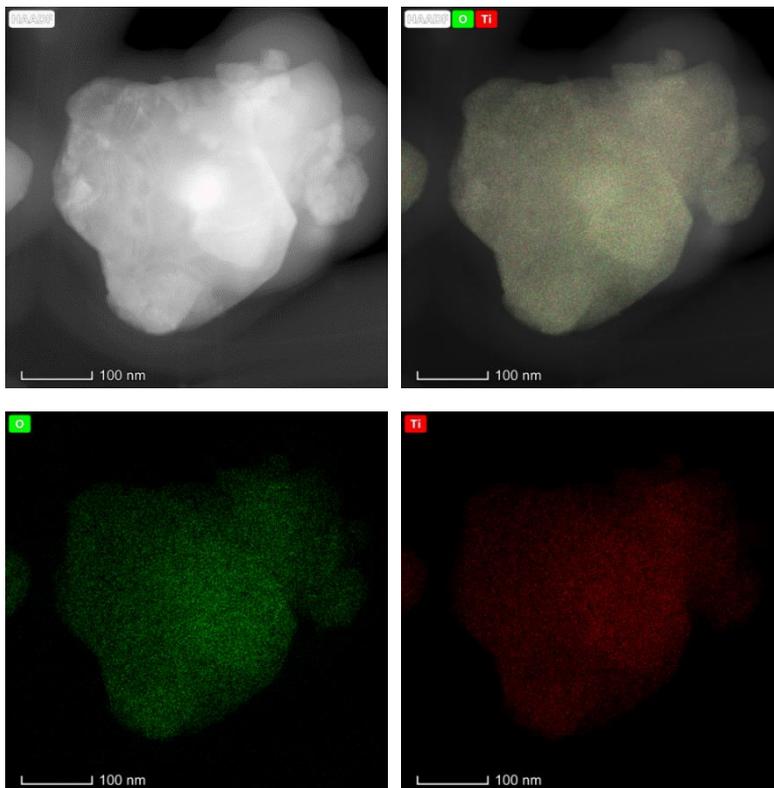**Fig. 6.** Elemental mapping of $Li_4Ti_5O_{12}$

Fig. 7 shows the cyclic voltammograms of $Li_4Ti_5O_{12}$ electrode sintered at 900 °C recorded at different scan rates (i.e. 5, 10, 20, 50, and 100 mV s^{-1}) in the potential window of −0.3 to +0.5 V. The quasi-rectangular shape of the curves without obvious redox peaks, describes the capacitive behavior of the electrode with non-faradic contribution. In general, the scan rate can be analyzed by using the power law ($I = AV^b$, where I is the current (A), A and b are arbitrary coefficients and V is potential scan rate) and the estimated value of " b" in the present study is 0.91 vs Li/Li$^+$ representing that the charge storage is mostly via surface capacitance effect. The high surface to volume ratio due to low particle size leads to store more number of charges on the surface of the electrodes. The integral area of the CV curve is increased with increasing the scan rate. However, the shape of the curve holds good even at high scan rates signifying the structural stability of $Li_4Ti_5O_{12}$ electrode.

The GCD curves recorded in the potential window of -0.3 V to 0.5 V and at current densities of 0.5, 1.0, and 2 A/g are shown in Fig.8. The nearly linear and symmetrical charge/discharge curves indicate that absorption and desorption processes of the electrode materials are good reversible, which is the characteristic of capacitive nature. The rapid increase/decrease in potential of GCD curves during the initial process of charging/discharging is due to the absorption Li anions on the surface which leads to form double layer capacitance.
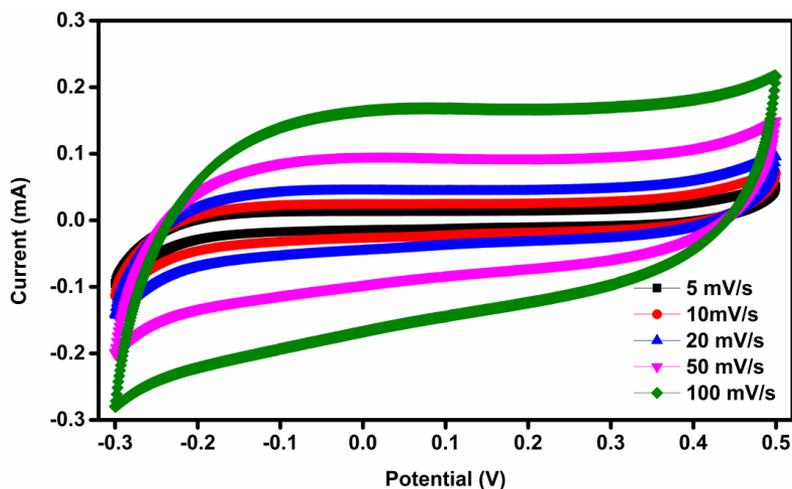
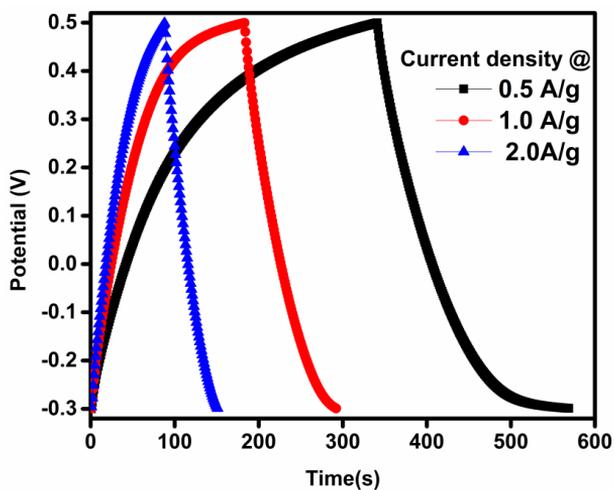**Fig. 7.** Cyclic voltammograms of $Li_4Ti_5O_{12}$ electrode recorded at different scan rates

Fig. 8. Galvano static charge–discharge curves of $Li_4Ti_5O_{12}$

Thereafter, a slow rate of change has been observed up to the plateau region. The observation of nearly rectangular shape of CV and symmetrical GCD curves represent the characteristic of capacitive behavior. The specific capacitance C_s can be calculated from GCD curves using the following relation:

$$C_s = \frac{i.\nabla t}{m.\nabla V} \qquad (2)$$

Where:
∇t = discharge time;
∇V = potential window;
i = current applied;
m = mass of the active material on the electrode.

The calculated specific capacitance of $Li_4Ti_5O_{12}$ electrode was found to be 265, 194, 139 F/g at current densities of 0.5, 1.0, 2 A/g, respectively. At low current densities, plenty of Li ions are accessible with cubical surface of the $Li_4Ti_5O_{12}$ electrode which provides high specific capacitance and vice versa [27, 28].

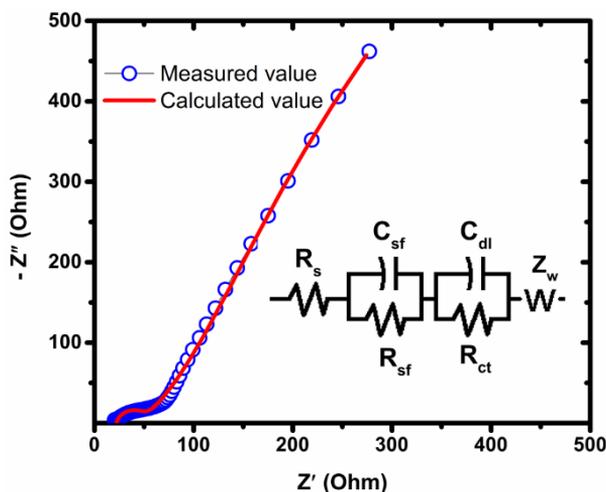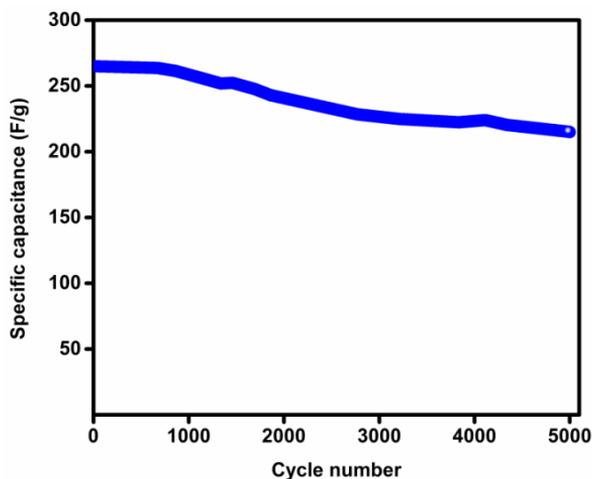**Fig. 9.** Nyquist plot of nanocrystalline $Li_4Ti_5O_{12}$ as electrode

Fig. 10. Cycling stability of $Li_4Ti_5O_{12}$ as electrode

The Nyquist plot of $Li_4Ti_5O_{12}$ electrode in the frequency range 1.0 Hz - 1.0 M Hz using 1 mol /L Li_2SO_4 aqueous solution as electrolyte was recorded and is shown in Fig. 9. The estimated ohmic resistance of the electrode (R_s) from intercept of X-axis at high frequency region is 22 Ω. The observed depressed semicircle in the high and intermediate frequency region is originated from the charge transfer resistance (R_{ct}). The calculated charge transfer resistance (R_{ct}) is about 51 Ω. The slightly inclined line at about $\theta = 65°$ (low-frequency region) is ascribed to the Warburg impedance corresponding to the diffusion control process of lithium ions through the electrode-electrolyte interface. Also, Nyquist plot is equipped with an analogous R(CR)(CR)W circuit model using ZSim Demo 3.20d and depict in Fig. 9. It is well fitted to the equivalent circuit with

a chi square value of 5.07×10^{-3}. Fig. 10 shows the cycle stability of LTO electrode recorded at 0.5 A/g. The synthesized electrode delivered a discharge capacitance of 265 F/g at first cycle and retained 81 % capacitance even after 5000 cycles. The excellent electrochemical performance of phase pure $Li_4Ti_5O_{12}$ electrode is because of low particle size, good crystallinity along with high surface to volume ratio.

Conclusions

The solid state reaction method has been employed for the synthesis of phase pure Nanocrystalline spinel $Li_4Ti_5O_{12}$ using anatase TiO_2 and Li_2CO_3 raw precursors. The structure, morphology, thermal, compositional and electrochemical properties of $Li_4Ti_5O_{12}$ electrode were characterized through XRD, TG, TEM, SEM with EDS, and Electrochemical analyzer, respectively. The XRD, TEM and Thermal studies confirmed the formation $Li_4Ti_5O_{12}$ with cubic spinel structure when sintered at a temperature of 900 °C without any impurity phases. The SEM images of $Li_4Ti_5O_{12}$ powder synthesized at 900ºC exhibited the formation of uniformly distributed grains and each grain is composed of several crystallites. The TEM analysis revealed cubic structure with a d- spacing of 0.48 nm corresponding to the (111) orientation of XRD spectrum of $Li_4Ti_5O_{12}$ phase. Therefore, the synthesized phase pure $Li_4Ti_5O_{12}$ electrode exhibited a good discharge specific capacitance of 265 F/g at current density of 0.5 A/g with excellent cycling stability (81%) after 5000 cycles and considered to be a promising electrode for supercapacitor applications.

References

[1] P. Rosaiah, j. Zhu, o. M. Hussain, y. Qiu, *synthesis of flower-like reduced graphene oxide–mn₃o₄ nanocomposite electrodes for supercapacitors*, **Appl. Phys. A 124** , 597, 2018, pp. 1-9.

[2] A. Lakshmi Narayana, M. Dhananjaya, N. Guru Prakash, O. M. Hussain, C. M. Julien, *Nanocrystalline Li_2TiO_3 electrodes for supercapattery application,* **Ionics 23**, 2017, pp. 3419-3428.

[3] M. Dhananjaya, A. Lakshmi Narayana, N. Guru Prakash, P. Rosaiah, O. M. Hussain, *Intertwining network structured V_nO_{2n+1}-CNT/GO nanocomposite electrodes for supercapacitors,* **Mater. Chem. Phys. 237,** 2019, 121825.

[4] A. Lakshmi Narayana, M. Dhananjaya, N. Guru Prakash, A. Mauger, C. M. Julien, O. M. Hussain, *Li_2TiO_3/Ni foam composite as high-performance electrode for energy storage and conversion,* **Heliyon 5(7)**, 2019, e02060.

[5] P. Jeevan Kumar, K. Jayanth Babu, O. M. Hussain, *Enhanced electrochemical properties of as grown $LiCoO_2$ film cathodes: Influence of silicon substrate surface texturing,* **Mater. Chem. Phys. 143**, 2014, 536.

[6] B. Purusottam Reddy, K. Sivajee Ganesh, O. M. Hussain, *Growth, microstructure and supercapacitive performance of copper oxide thin films prepared by RF magnetron sputtering*, **Appl. Phys. A Mater. Sci. Process. 122,** 2016, 128.

[7] N. Guru Prakash, M. Dhananjaya, A. Lakshmi Narayana, Hussen Maseed, V. V.S.S Srikanth, O. M. Hussain, *Improved electrochemical performance of rGO-wrapped MoO_3 nanocomposite for supercapacitors*, **Appl. Phys. A 125** (2019) 488.

[8] M. Khairy, K. Faisal, M.A. Mousa, *High-performance hybrid supercapacitor based on pure and doped $Li_4 Ti_5 O_{12}$ and graphene,* **J Solid State Electrochem 21**, 2017, pp. 873-882.

[9] C. V. Ramana, S Utsunomiya, R. C. Ewing, U. Beckeri, K. Zaghib, C. M. Julien, *Synthesis, Structure, and Electrochemical Properties of $Li_4Ti_5O_{12}$,* **Mater. Res. Soc. Symp. Proc. 973**, 2007, BB05-09.

[10] Subramanian Natarajan, Krishnan Subramanyan, Vanchiappan Aravindan, *Focus on Spinel Li₄Ti₅O₁₂ as Insertion Type Anode for High-Performance Na-Ion Batteries*, **Small 15(49)**, 2019, 1904484.

[11] Jong Hyun Kim, Jung Rag Yoon, *Preparation and characterization of Li₄Ti₅O₁₂ synthesized using hydrogen titanate nanowire for hybrid super capacitor,* **J. Adv. ceram. 2(3)**, 2013, pp. 285-290.

[12] Byunggwan Lee, J. R. Yoon, *Preparation and characteristics of Li₄Ti₅O₁₂ with various dopants as anode electrode for hybrid supercapacitor,* **Curr. Appl. Phys., 13(7)**, 2013, pp. 1350-1353.

[13] J. Ni, L. Yang, H. Yang, L. Gao, *A high-performance hybrid supercapacitor with Li₄Ti₅O₁₂-C nano-composite prepared by in situ and ex situ carbon modification*, **J Solid State Electrochem 16**, 2012, pp. 2791-2796.

[14] S. Stewart, P. Albertus, V. Srinivasan, I. Plitz, N. Pereira, G. Amatucci, J. Newman, *Optimizing the performance of lithium titanate spinel paired with activated carbon or iron phosphate*, **J Electrochem. Soc, 155(3),** 2008, pp. A253-A261.

[15] Xiangcheng Sun, Pavle V, Radovanovic, Bo Cui, *Advances in spinel Li₄Ti₅O₁₂ anode materials for lithium-ion batteries*, **New J. Chem., 39**, 2015, pp. 38-63.

[16] Ali Ghorbani Kashkooli, Gregory Lui, Siamak Farhad, Dong Un Lee, Kun Feng, Aiping Yu, Zhongwei Chen, *Nano-particle size effect on the performance of Li₄Ti₅O₁₂ spinel*, **Electrochim. Acta, 196**, 2016, pp. 33-40.

[17] Juan Li, Yong Li Jin, Xiao-Gang Zhang, Hui Yang, *Microwave solid-state synthesis of spinel Li₄Ti₅O₁₂ nanocrystallites as anode material for lithium-ion batteries,* **Solid State Ion., 178** , 2007, pp. 1590-1594.

[18] Kai Leng, Fan Zhang, Long Zhang, Tengfei Zhang, Yingpeng Wu, Yanhong Lu, Yi Huang, Yongsheng Chen, *Graphene-based Li-ion hybrid supercapacitors with ultrahigh performance*, **Nano Res. 6(8)**, 2013, pp. 581-592.

[19] SiXu Deng, JingWen Li, ShiBing Sun, Hao Wang, JingBing Liu, Hui Yan, *Synthesis and electrochemical properties of Li₄Ti₅O₁₂ spheres and its application for hybrid supercapacitors,* **Electrochim. Acta, 146,** 2014, pp. 37-43.

[20] L-L. Xing, K-J. Huang, S-X. Cao, H. Pang, *Chestnut shell-like Li₄Ti₅O₁₂ hollow spheres for high-performance aqueous asymmetric supercapacitors*, **Chem. Eng. J. 332**, 2018, pp. 253-259.

[21] Yanbin Shen, Martin Sondergaard, Mogens Christensen, Steinar Birgisson, Bo B. Iversen, *Solid State Formation Mechanism of Li₄Ti₅O₁₂ from an Anatase TiO₂ Source*, **Chem. Mater., 26(12)**, 2014, pp. 3679-3686.

[22] I. Veljkovic, D. Poleti, L. J. Karanovic, M. Zdujic, G. Brankovic, *Solid State Synthesis of Extra Phase-Pure Li₄Ti₅O₁₂ Spinel,* **Sci. Sinter. 43**, 2011, pp. 343-351.

[23] Yin, S. Y., Song, L., Wang, X. Y., Zhang, M. F., Zhang, K. L., Zhang, Y. X., *Synthesis of spinel Li₄Ti₅O₁₂ anode material by a modified rheological phase reaction*, **Electrochim. Acta, 54**, 2009, 5629-5633.

[24] M. Kitta, K. Kuratani, M. Tabuchi, N. Takeichi, T. Akita, T. Kiyobayashi, M. Kohyama, *Irreversible structural change of a spinel Li₄Ti₅O₁₂ particle via Na insertion-extraction cycles of a sodium-ion battery*, **Electrochim. Acta, 148**, 2014, pp. 175-179.

[25] B. Vikram Babu, K. Vijaya Babu, G. Tewodros Aregai, L. Seeta Devi, B. Madhavi Latha, M. Sushma Reddi, K. Samatha, V. Veeraiah, *Structural and electrical properties of Li₄Ti₅O₁₂ anode material for lithium-ion batteries,* **Results Phys. 9**, 2018, pp. 284-289.

[26] Bhatti, H. S., Anjum, D. H., Ullah, S., Ahmed, B., Habib, A., Karim, A., Hasanain, S. K., *Electrochemical Characteristics and Li+ Ion Intercalation Kinetics of Dual-Phase*

Li₄Ti₅O₁₂/Li₂TiO₃ Composite in the Voltage Range 0–3 V, **J. Phys. Chem. C 120(18)**, 2016, pp.9553-9561.

[27] Na Li, Tao Mei, Younchun Zhu, Linlin Wang, Jianwen liang, Xing Zheng, Yitai Qiam, Kaibin Tang, *Hydrothermal synthesis of layered Li₁.₈₁H₀.₁₉Ti₂O₅.xH₂O nanosheets and their transformation to single crystalline Li₄Ti₅O₁₂ nanosheets as the anode materials for Li-ion batteries,* **Cryst Eng Comm. 14,** 2012, pp. 6435 – 6440.

[28] M. Dhananjaya, N. Guruprakash, A. Lakshmi Narayana, O. M. Hussain, *Microstructural and supercapacitive properties of one dimensional vanadium pentoxide nanowires synthesized by hydrothermal method*, **Appl. Phys. A. 124**, 2018, PP. 185-91.